Intramolecular Reaction Rates of Flexible Polymers. 1. Simulation Results and the Classical Theory

Marta Ortiz-Repiso, Juan J. Freire, and Antonio Rey*

Depto. Química Física I, Facultad de Ciencias Químicas, Universidad Complutense, 28040 Madrid, Spain

Received February 19, 1998; Revised Manuscript Received August 31, 1998

ABSTRACT: We have used a Brownian dynamics numerical algorithm to simulate reversible intramolecular reactions taking place in flexible polymer chains in dilute solutions. The simulations are based on the Gaussian chain model, with the possibility of including long range interactions to mimic excluded volume conditions. Hydrodynamic interactions are considered at different levels of detail. We have extended our previous study of end-to-end cyclizations to longer chains and added the analysis of cyclization processes involving inner units. The numerical results of the cyclization rate constants are systematically compared with the results of the classical cyclization theory of Wilemski and Fixman, to better understand the effect of the theoretical approximations. The conclusions previously described for shorter chains are confirmed in general, though in some cases they become slightly corrected by the more accurate results of this work. In addition, we have extended our analysis to end-to-interior and interior-to-interior intramolecular processes.

1. Introduction

There are several physical properties and experimental techniques which allow the study of the dynamic behavior of polymer chains in dilute solution. These include the analysis of intramolecular reactions,[1] which take place when two or more active groups are located on the same chain, with a reasonable separation among them along the chain contour. These groups can react if the movements or the conformation of the chain brings them close enough in space. Depending on the system, the result of the reaction may be the formation of a temporal or permanent closed loop or just a physical or chemical change in the involved groups, without any change in the chain topology.

Intrapolymeric reactions (also termed *cyclizations*) have been also the aim of a detailed theoretical analysis. This was pioneered by the work of Wilemski and Fixman[2,3] (WF). They used the Rouse−Zimm polymer dynamics model to relate the rate constant of the end-to-end cyclization process to the longest relaxation time of the chain. The original theory could be only directly applied to infinitely long chains in the unperturbed or Θ regime. It also included several approximations, mainly the following: (a) the reaction is diffusion-controlled; (b) the hydrodynamic interactions (HI) between chain units are described through the preaveraging approximation;[4] (c) the theory considers a sink operator to represent how the distribution function is spatially distorted as time grows, a specific form for this distortion being assumed (*sink closure approximation*).

The WF theory was reformulated for finite chains and widely spread in the treatment of experimental data mainly by Perico and Cuniberti[5,6] (PC). They also included the possibility that the reaction is not always diffusion-controlled (DC). The kinetic rate constant in the case of chemical control is calculated from the DC constant, after dividing it by the effective concentration of one reactive group in the neighborhood of the other. The theory, however, uses this latter constant mainly as a normalized version of the former. Thus, we will only compute in this work the theoretical estimations of the DC limit of the cyclization constants (i.e., those corresponding to a fast reaction at every encounter of the active groups) in order to compare them with the simulation results.

Continuing the WF−PC theory, Perico and Beggiato extended this work to include the possibility that the reaction takes place between groups located at positions different from the chain ends.[7] However, the approximations mentioned above were maintained in these refinements.

Given this situation, we began some time ago to check the theory against simulation results. We computed Brownian dynamics simulations of relatively short Gaussian chains with a simple numerical algorithm.[8] Later, we extended these calculations to good solvent conditions.[9] In both cases we got significant differences between the simulation rate constants and the theoretically predicted results.

Here, we try to extend those comparisons to longer chains, and to the case were internal units are considered as part of the intramolecular reaction. Specifically, we have computed end-to-end (case I), end-to-interior (case II) and interior-to-interior (case III) cyclization rates. In the latter case, the reactive groups are symmetrically located in the chain; i.e., there are two identical tails from the reactive groups to the chain ends. The WF theory, through the PC formalism, can provide results for the three cases considered, though some intermediate numerical results have to be introduced in the analytical expressions under certain conditions. However, this will allow us the possibility of a better evaluation of the different approximations included in the theory.

More recently, scaling laws based on the renormalization group theory have been predicted for the rate constants of intramolecular reactions.[10,11] We shall compare our simulation results with this theory in the companion paper.

* To whom all correspondence should be addressed.

10.1021/ma980254t CCC: $15.00
Published on Web 10/30/1998

2. Model and Methods

As we have done in previous works,[8,9] we consider a bead and spring linear chain model whose root-mean-square distance between neighbor units is b. When excluded volume (EV) interactions are considered, we add a soft intramolecular potential between nonneighbor units whose effects are in good agreement with theoretical predictions and experimental observations for these good solvent conditions.[12]

We have computed numerical Brownian dynamics trajectories for isolated model chains following a modification of the classical Ermak and McCammon algorithm,[13] in which a pseudo second-order algorithm is employed.[14] We have kept the fundamental time-step interval of the algorithm in our standard reduced value $\Delta t^* = 0.01$, though the higher order algorithm would allow us to use a larger value. Since, in addition, we have considerably extended the number of steps in the trajectories, we hope that the simulation results reported here have better quality and more numerical accuracy than our previous results of the same properties. The same algorithm has been very recently used to consider the effect of chain impenetrability on polymer dynamics and cyclization rates, using different models without hydrodynamic interactions.[15]

The simulation algorithm calculates the different coordinates of the model units at every time step. This calculation requires obtaining the intramolecular forces defined by the model and the chain diffusion tensor (describing the hydrodynamic interactions, HI, considered). The HI are controlled by a parameter $h^* = (\pi/3)^{1/2}(\sigma/b)$, where σ represents the frictional radius of the model units. A value $h^* = 0$ corresponds to free-draining (neglect of HI) conditions, while $h^* = 0.25$ describes the partial draining conditions, both for approximated (preaveraged) and rigorous (fluctuating) HI.

The length of the computed trajectories depends on N, the number of chain units, and on the conditions studied. For example, excluded volume conditions make the cyclization process more difficult, which obliges us to compute longer trajectories in order to find a statistically significant number of cyclization events. Thus, the number of Brownian dynamics steps ranges from 75×10^3 for the shortest chains ($N = 10$) without EV up to 4×10^6 for the longest ($N = 75, 145$) with EV. Also, since these trajectories may not be in some occasions long enough for the slow dynamic processes considered here, five independent trajectories have been computed for every N and set of conditions. The results presented correspond to the average over these trajectories. The CPU time required in each individual trajectory ranges from less than 1 h to about 15 days on a DEC 433au workstation.

To compute the reaction rates, we first calculate the probability $\Phi(\tau)$ that two reactive groups remain active (i.e., they have not reacted) over the time period τ. We define that the groups have reacted if the distance between them in a given trajectory step is smaller than a fixed value of the capture radius, R_0. Details for the calculation and normalization of $\Phi(\tau)$ are given in our previous work.[8,9]

Since our cyclization process assumes only the proximity of the designed reactive groups, we can use a given trajectory to simultaneously compute the probabilities $\Phi(\tau)$ of different intramolecular reactions. Namely, we have computed in every trajectory the end-to-end cyclization and, for all but the shortest chains, end-to-interior and interior-to-interior cyclization processes. In the end-to-interior case, we use both chain ends and average their results.

From the probability functions we get the cyclization rate constants k_1, assuming a single-exponential behavior of $\Phi(\tau)$. This behavior, first predicted by the WF theory (though strictly the theory predicts a multiexponential behavior, the first term accounts for over 99.9% of the probability), has been confirmed by our results in all the cases.

The calculation of the rate constants based on the WF method through the PC formalism is accomplished by numerically solving the integral equation[3,5,6]

$$k_1 = \left[\int_0^\infty \left(\frac{k(\tau)}{k_\infty} - 1\right) \exp(k_1\tau)\, d\tau\right]^{-1} \quad (1)$$

where

$$k(\tau) = \mathrm{erf}[Z(\tau)] - \left(\frac{2}{\pi^{1/2}}\right) Z(\tau) \exp[-Z^2(\tau)] \quad (2)$$

$$Z(\tau) = \gamma_R [1 - \rho^2(\tau)]^{-1/2} \quad (3)$$

$$\gamma_R = \left(\frac{3}{2}\right)^{1/2} \frac{R_0}{\langle r^2\rangle^{1/2}} \quad (4)$$

(k_∞ is $k(\tau)$ for $\tau \to \infty$). $\langle r^2\rangle$ is the mean quadratic distance between the two considered reactive beads. Under Θ conditions, $\langle r^2\rangle = (S - 1)b^2$, S being the number of units between the two reacting groups. In the presence of excluded volume repulsive interactions, this value has been computed from the simulations.

The function $\rho(\tau)$ in eq 3 is the time correlation function for the vector $\boldsymbol{r}$ joining the reactive groups

$$\rho(\tau) = \langle \mathbf{r}(t)\cdot\mathbf{r}(t+\tau)\rangle / \langle r^2\rangle \quad (5)$$

which can be evaluated analytically only for unperturbed chains under free draining conditions or with the preaveraged HI approximation.[5,6] Since this merely covers a fraction of the conditions studied in this work, we have numerically evaluated this function from the trajectories in all the cases computed with either EV or with fluctuating hydrodynamic interactions. To properly use this numerical function in eq 3, we showed previously[9] that it can be adequately fitted to a biexponential curve, with the first term accounting for most of the decay, and an exponent very close to the longest relaxation time of the chain, in a Rouse normal mode scheme. The same result is still valid here for case I (end-to-end) processes in considerably longer chains. However, in cases II and III we have always needed three exponential terms to reproduce the correlation function behavior. Thus, we use a fitting function of the form

$$\rho(\tau^*) = A_1 \exp(-B_1\tau^*) + A_2 \exp(-B_2\tau^*) + (1 - A_1 - A_2) \exp(-B_3\tau^*) \quad (6)$$

where A_1, A_2, B_1, B_2, and B_3 are adjustable parameters. The star indicates the use of reduced units, which for time are $t^* = t[k_B T/(6\pi\eta_0\sigma b^2)]$, η_0 being the solvent viscosity. Precisely, the cyclization rate constants have units of reciprocal time. They will be expressed in the same reduced units all along this work.

Before presenting the results corresponding to the cyclization processes, we can check the accuracy of our simulation procedures by comparing the results for the correlation function $\rho(\tau)$ obtained from the trajectories with those analytically computed, when this is possible. As a matter of fact, this check was previously performed in case I cyclizations, for unperturbed chains in free draining conditions and with preaveraged HI (see Figure 1 in ref 9). As a further example, we present in Figure 1 a few cases of the correlation function for end-to-interior and interior-to-interior groups, for a long unperturbed chain under free draining conditions. The excellent agreement between theory and simulation is found in all the cases when this comparison is possible. Of course, there is a small amount of fluctuating noise in the numerical results, especially at long times. This has no effect in the calculation of the rate constants, when they have to be computed from numerical estimates of $\rho(\tau)$. The fitting procedure described above completely eliminates this problem. As a matter of fact, if such a fitting is performed on the simulation data of Figure 1, the fitted curve is virtually undistinguishable from the theoretical curve (and therefore is not included in the figure). That means that the theoretical estimations we obtain for the rate constants according to eqs 1−4 are the same if we use the analytical expression for $\rho(\tau)$ as if we use the correlation

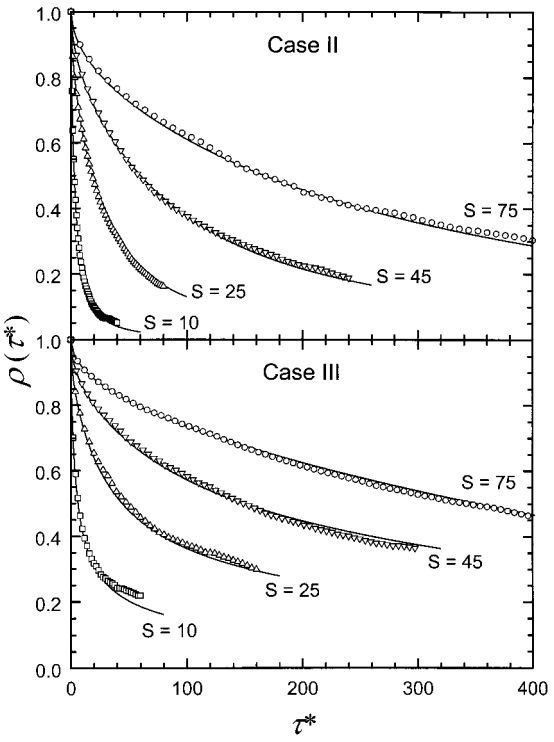

Figure 1. Normalized correlation function for the vector joining the positions of the two reactive groups, for unperturbed chains with $N = 145$ and free draining conditions. The symbols correspond to the function numerically computed from the simulation trajectories, while the solid line is calculated from the theoretical expression.[6,7]

function from the trajectories. Overall, the comparison of Figure 1 clearly shows that the dynamic models underlying the WF−PC theory and our simulation are equivalent. This is an important point prior to the comparison of the cyclization rate constants obtained from both methods.

3. Results and Discussion

Figure 2 shows an example of the cyclization probability functions $\Phi(\tau)$ for different chain lengths N, two capture radius R_0 (reduced by the fundamental length unit of our model, b), and different considerations of solvent quality and HI. This figure allows us a first qualitative description of the factors influencing the cyclization process. The longer the chain, the slower the process, as indicated by a slower decrease of the probability function. Obtaining the exact dependence of the cyclization constants on N is the main aim of the companion paper. The effect of the radius of capture R_0, as predicted by the WF theory, is also evident: a larger value of R_0 results in a faster decay of $\Phi(\tau)$, whatever the value of N. This is an expected result, since the process is made easier when the reactive volume around the active groups increases, a fact which has been experimentally verified.[16,17]

The effect of excluded volume is exactly the opposite: cyclizations in a good solvent are clearly slowed respect to their situation in a Θ solvent. Again, this is not a surprise, since the effective repulsions appearing between nonneighbor units in excluded volume conditions make it more difficult for the reactive groups to reach the short distance necessary for the cyclization to take place. Its effect on the probability $\Phi(\tau)$ is considerably more important than the consideration of HI. This latter property has slightly different effects depending on the reduced capture radius R_0/b, as can be observed in Figure 2. Its effect will become clearer from the values of the reaction rate constants k_1 we will shortly report. However, the effect of HI and their approximations in end-to-end cyclizations has been the aim of previous work,[8,9] and it will be only marginally analyzed here.

For cases II and III, involving inner groups in the chains, the qualitative conclusions are the same we have commented for case I, and we do not explicitly include the corresponding graphics in this work.

As stated in the Introduction, the functions plotted in Figure 2 can be easily fitted to a single-exponential function. The corresponding exponent is the rate constant k_1 obtained from the simulations, which we compare now with the predictions of the WF theory.

3.1. Approximate Treatment of Hydrodynamic Interactions. We have already said that, strictly speaking, analytical results for k_1 can be only obtained for processes without EV, in free draining conditions (FD) or under the approximation of preaveraged hydrodynamic interactions (PHI). (These are the only situations in which the correlation function $\rho(\tau)$ can be, and has been, evaluated without using the trajectory data.) Thus, we begin our presentation of results with these two situations, whose computed rate constants for case I processes are included in Table 1. The effect of HI on cyclization rates has been already discussed.[5] Therefore, we will directly focus our discussion in the comparison between simulation and theoretical results under the same conditions. To favor this comparison, the ratio of simulation to theoretical results is plotted vs the number of chain units in Figure 3. In previous work,[9] we had observed that this ratio was close to unity for short chains and $R_0/b = 0.5$, but was always larger than unity for the larger value $R_0/b = 1.0$. Our present results seem to confirm this latter trend for long chains, without any clear influence of the capture radius on the ratio of the results. This ratio slightly grows with N, and from the curves in Figure 3 one could guess that it tends toward some short of plateau. This would imply that the simulation results for the end-to-end cyclization rate constants for long chains are about 100% larger than the theoretical estimations in free draining conditions, while this value is "only" about 60% when HI is considered through the preaveraged approximation. All these discrepancies can be attributed to the effects of the sink closure and other approximations in the WF method, but not to the treatment of HI. This, together with the possible effect of the reversibility of the cyclizations implicit in our calculation of $\Phi(\tau)$ from the trajectories, has been previously discussed.[9] The results reported here for longer chains and with a better simulation algorithm corroborate our previous conclusions.

To check whether these observations can be also extended to intramolecular reactions involving internal units, we present and discuss now the results for the same type of systems (unperturbed chains, in FD or PHI conditions) in end-to-interior (case II) and interior-to-interior (case III) processes. The results are presented in Tables 2 and 3, respectively. Since this type of simulation results has not been, in the best of our knowledge, presented before, we shall discuss their novel features here.

First, from these data, and those in Table 1, we can see that, for identical chain fragments (equal values of S, or N in cyclization case I), the rate constant is smaller

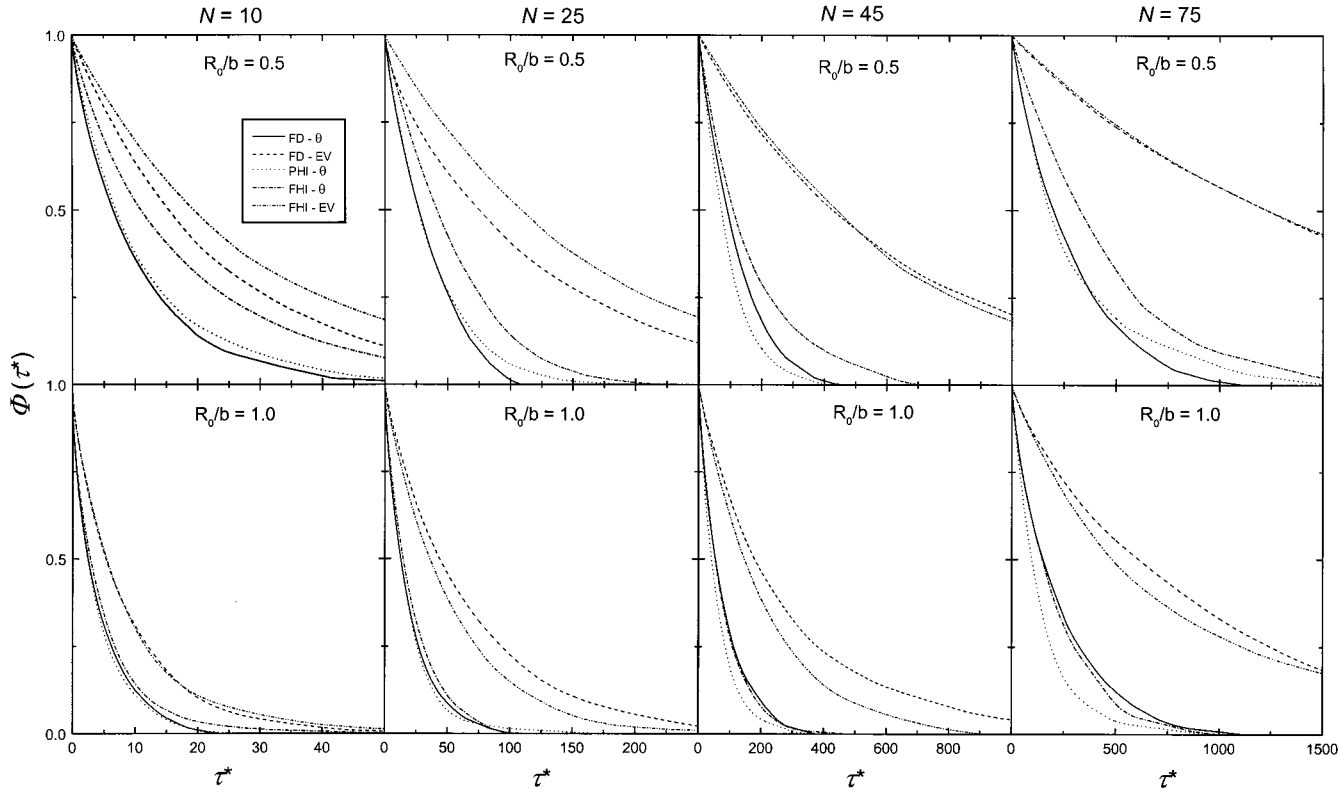

Figure 2. Case I cyclization probability functions for different chain lengths, N, capture radius, R_0, and simulation conditions. Key: FD, free draining; PHI, preaveraged hydrodynamic interactions; FHI, fluctuating hydrodynamic interactions; Θ, unperturbed conditions; EV, excluded volume.

Table 1. End-to-End Cyclization Constants (in Reduced Units) Obtained from the Simulations, k_1^{BD}, and from the Theoretical Estimates, k_1^{WF}, for Unperturbed (Θ) Chains under Free Draining (FD) and Preaveraged Hydrodynamic Interaction (PHI) Conditions

		FD − Θ		PHI − Θ	
R_0/b	N	$10^2(k_1^{BD})^*$	$10^2(k_1^{WF})^*$	$10^2(k_1^{BD})^*$	$10^2(k_1^{WF})^*$
0.5	10	9.37 ± 0.01	8.39	9.7 ± 0.2	8.26
	25	2.52 ± 0.04	1.39	2.55 ± 0.03	1.77
	45	0.8 ± 0.1	0.39	0.92 ± 0.07	0.58
	75	0.35 ± 0.03	0.15	0.34 ± 0.05	0.22
1.0	10	20.5 ± 0.6	14.7	20.1 ± 0.5	15.7
	25	4.8 ± 0.2	2.50	4.7 ± 0.3	3.10
	45	1.2 ± 0.2	0.63	1.7 ± 0.1	1.06
	75	0.7 ± 0.1	0.42	0.75 ± 0.06	0.41

in case II than in case I and is even smaller in case III. Qualitatively, this has to be understood as a slower process when the reactive groups have to drag a tail of $(N - S)$ units (in case II) or two tails of $(N - S)/2$ units (case III). As the tail or tails become longer, however, the units situated along the tails that are remote from the active groups have little influence on the cooperative motions of the polymer that bring about the cyclization of the fragment of S units, and a limiting value is reached. The rate constant depends on S, but it is independent of N. This fact has been very recently observed experimentally.[18] In the companion paper we will further discuss the possibility to extract this limiting value from our simulation data.

The theoretical estimations of k_1 show also this behavior, as had been previously pointed out.[7] We have to remember that, to get these estimations, one has to include in the calculation the correlation function $\rho(\tau)$ (in its analytical form, for this particular case). This correlation function shows the same tail effect mentioned in the previous paragraph, an effect which translates into the rate constants.

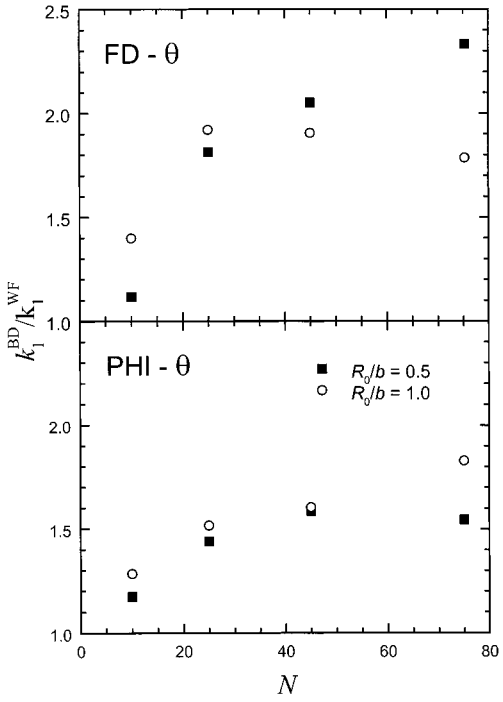

Figure 3. Ratio of case I cyclization constants obtained from simulations, k_1^{BD}, and from the theoretical estimates, k_1^{WF}, for unperturbed (Θ) chains under free draining (FD) and preaveraged hydrodynamic interaction (PHI) conditions.

The influence of HI in these constants can be also appreciated. In general, the consideration of HI, even under the preaveraging approximation, makes the rate

Table 2. End-to-Interior (Case II) Cyclization Constants (in Reduced Units) Obtained from the Simulations, k_1^{BD}, and from the Theoretical Estimates, k_1^{WF}, for Unperturbed (Θ) Chains under Free Draining (FD) and Preaveraged Hydrodynamic Interaction (PHI) Conditions, Where *S* Represents the Number of Segments in the Chain Fragment Separating the Reacting Units

			FD − Θ		PHI − Θ	
R_0/b	S	N	$10^2(k_1^{BD})^*$	$10^2(k_1^{WF})^*$	$10^2(k_1^{BD})^*$	$10^2(k_1^{WF})^*$
0.5	10	25	9.1 ± 0.3	6.12	8.9 ± 0.6	7.16
		45	8.3 ± 0.8	5.28	9.2 ± 0.5	6.90
		75	7.6 ± 0.2	5.47	8.36 ± 0.08	6.96
		145	7.83 ± 0.01	5.43		
1.0	10	25	16.5 ± 0.2	8.81	20.4 ± 0.8	13.1
		45	16.9 ± 0.6	8.70	18.5 ± 0.2	11.7
		75	15.5 ± 0.1	8.14	17.85 ± 0.09	11.6
		145	15.5 ± 0.3	7.83		
0.5	25	45	1.34 ± 0.08	0.86	1.71 ± 0.04	1.50
		75	1.39 ± 0.01	0.84	1.68 ± 0.05	1.31
		145	1.20 ± 0.06	0.74		
1.0	25	45	2.5 ± 0.1	1.41	3.51 ± 0.02	2.42
		75	2.4 ± 0.1	1.29	3.48 ± 0.02	2.20
		145	2.09 ± 0.03	1.20		
0.5	45	75	0.49 ± 0.04	0.28	0.67 ± 0.02	0.56
		145	0.50 ± 0.02	0.27		
1.0	45	75	0.75 ± 0.05	0.40	1.32 ± 0.02	0.91
		145	0.62 ± 0.06	0.35		
0.5	75	145	0.265 ± 0.006	0.13		
1.0	75	145	0.30 ± 0.04	0.16		

Table 3. Interior-to-Interior (Case III) Cyclization Constants (in Reduced Units) Obtained from the Simulations, k_1^{BD}, and from the Theoretical Estimates, k_1^{WF}, for Unperturbed (Θ) Chains under Free Draining (FD) and Preaveraged Hydrodynamic Interaction (PHI) Conditions Where *S* Represents the Number of Segments in the Chain Fragment Separating the Reacting Units

			FD − Θ		PHI − Θ	
R_0/b	S	N	$10^2(k_1^{BD})^*$	$10^2(k_1^{WF})^*$	$10^2(k_1^{BD})^*$	$10^2(k_1^{WF})^*$
0.5	10	25	6.75 ± 0.05	3.80	7.5 ± 0.5	5.90
		45	5.75 ± 0.05	2.31	6.4 ± 0.5	4.61
		75	5.4 ± 0.1	2.30	6.8 ± 0.1	3.81
		145	5.15 ± 0.05	1.93		
1.0	10	25	13 ± 1	5.45	15.0 ± 0.8	9.92
		45	11.2 ± 0.5	4.80	13.4 ± 0.2	8.91
		75	9.3 ± 0.2	4.20	12.0 ± 0.5	9.32
		145	8.6 ± 0.4	3.44		
0.5	25	45	0.91 ± 0.08	0.53	1.6 ± 0.2	1.30
		75	0.89 ± 0.07	0.46	1.4 ± 0.1	1.10
		145	0.82 ± 0.09	0.46		
1.0	25	45	1.7 ± 0.2	1.03	2.9 ± 0.3	1.82
		75	1.6 ± 0.1	0.59	2.8 ± 0.2	1.71
		145	1.37 ± 0.07	0.56		
0.5	45	75	0.31 ± 0.05	0.17	0.56 ± 0.02	0.51
		145	0.25 ± 0.05	0.15		
1.0	45	75	0.45 ± 0.06	0.22	0.94 ± 0.06	0.73
		145	0.39 ± 0.05	0.20		
0.5	75	145	0.103 ± 0.007	0.062		
1.0	75	145	0.23 ± 0.04	0.13		

constant larger than the free draining value. The effect is small for small values of S (short chain fragments), but easily appreciated for larger values of S. We can describe this feature taking into account that, under HI conditions, the friction of the chain units with the solvent is partially screened in the interior of the polymer coil, especially for long chains. This slightly speeds up the intramolecular dynamics of the chains, and therefore the cyclization dynamics.

Finally, we compare the simulation and theoretical results. Again, the latter are considerably smaller than the former for both cyclization cases, for both values of R_0, and under the different treatments of HI. Considering for every S the longer value of N in Tables 2 and 3, we obtain very similar conclusions to those from the end-to-end cyclizations. The ratios between simulation and theoretical results add up to values around two in FD conditions for case II (even slightly larger in case III) and around 1.5 under PHI conditions. Thus, our conclusion is that the theory underestimates the cyclization rates, no matter the position of the reactive groups, and this fact has nothing to do with the approximations involved in the treatment of hydrodynamic interactions.

Table 4. End-to-End Cyclization Constants (in Reduced Units) Obtained from the Simulations, k_1^{BD}, and from the Theoretical Estimates, k_1^{WF}, for Unperturbed (Θ) and Excluded Volume (EV) Chains with FHI

		FHI − Θ		FHI − EV	
R_0/b	N	$10^2(k_1^{BD})^*$	$10^2(k_1^{WF})^*$	$10^2(k_1^{BD})^*$	$10^2(k_1^{WF})^*$
0.5	10	6.9 ± 0.3	7.20	3.1 ± 0.2	6.05
	25	1.56 ± 0.08	1.60	0.58 ± 0.08	0.77
	45	0.59 ± 0.05	0.60	0.17 ± 0.02	0.28
	75	0.21 ± 0.02	0.22	0.056 ± 0.001	0.12
1.0	10	17 ± 1	15.5	11.3 ± 0.8	11.3
	25	4.2 ± 0.2	3.80	1.8 ± 0.1	1.63
	45	1.22 ± 0.08	1.20	0.42 ± 0.02	0.41
	75	0.45 ± 0.03	0.40	0.11 ± 0.02	0.10

3.2. Fluctuating Hydrodynamic Interactions. Since HI depends on the distance between the units in the macromolecule, its rigorous treatment includes its consideration as a fluctuating property (FHI). In this case, the correlation function $\rho(\tau)$ cannot be analytically evaluated. Therefore, all the results presented in this section, no matter whether they come from simulation or theory, use the function $\rho(\tau)$ calculated from the trajectories, which is fitted to a multiexponential function.

The results of the case I cyclization rate constants in unperturbed and excluded volume contitions are collected in Table 4. The effect of excluded volume is clearly appreciated, yielding smaller rate constants, in accordance with qualitative predictions[3,6,7] and experimental data.[1,19] The difference is larger the longer the chain, and it seems also more important for the larger value of the capture radius R_0.

The comparison between simulation and theoretical results is made easier by computing the ratio of both types of constants, as we have done with the results derived from simplified treatments of HI. This ratio is plotted in Figure 4. To help understanding the meaning of our new results, values for $N = 6$, 8, 11, 15, and 20, which had been previously reported,[9] are also included in the plots.

For $R_0/b = 1.0$, there is an impressive agreement between our new simulation data and theoretical results. The theory still underestimates the rate constants, but the difference never surmounts 10% for long chains. Even for short chains at unperturbed conditions, our result for $N = 10$ bears the same conclusion. Older results for short chains deviate from this trend, most probably reflecting the limited accuracy of the older simulation results. For $R_0/b = 0.5$ the situation is rather different. Both sets of results are still about the same under Θ conditions, but in a good solvent the simulation results are now considerably less (by about half) than the theoretical prediction. None of the cases in this figure shows any apparent trend with the chain length, as it could be observed to happen in Figure 3.

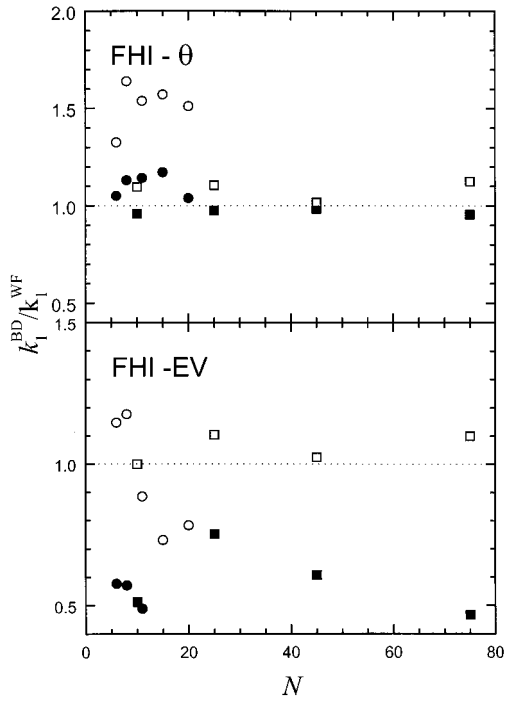

Figure 4. Ratio of case I cyclization constants obtained from simulations, k_1^{BD}, and from the theoretical estimates, k_1^{WF}, for unperturbed (Θ) and excluded volume (EV) chains with fluctuating hydrodynamic interactions (FHI). Solid symbols: $R_0/b = 0.5$. Open symbols: $R_0/b = 1.0$. Squares: new results of this work. Circles: results from data previously reported.[9]

To try to explain this different comparison of results between unperturbed and good solvent conditions, we have to remember once more the origin of the theoretical results we are using. They are still based on the WF−PC treatment (eqs 1−4), but with a correlation function $\rho(\tau)$ computed from the same trajectory used to extract the numerical estimation of the cyclization constant. Under Θ conditions this fact seems to be enough to compensate for other approximations present in the theory. This result, however, should be interpreted carefully. While the theoretical expressions could be still safely used to estimate the rate constants, it is necessary anyway to run the simulation in order to calculate the correlation function $\rho(\tau)$. Given this situation, one could proceed with the simulation alone to obtain the rate constant directly from the analysis of the cyclization probability function. The only practical point favoring the use of the theory, especially for the longest chains, is that one needs really huge trajectory lengths in order to properly compute $\Phi(\tau)$. On the other hand, a reasonable estimation of $\rho(\tau)$ can be calculated with shorter (though still long) trajectories, therefore lowering the computational cost of the full calculation.

When excluded volume interactions are considered, the equilibrium function characterizing chain statistics is seriously perturbed from its Gaussian form. Then, it is not clear whether the equations corresponding to the WF−PC theory are still valid. Their use with numerical values of $\rho(\tau)$ calculated from the trajectories can be only considered as an ad hoc approximation which, however, does not reproduce the simulation results, at least for a small capture radius. In the companion paper, we will explore the possibility that other approximations of the WF theory, namely the diffusion control, may not be adequate in systems with FHI and EV, which most probably will aid to explain the differences encountered for $R_0/b = 0.5$, and even pose some doubts on the coincidence found for $R_0/b = 1.0$. Thus, part of the discussion of this point will be deferred to the next paper.

Table 5. End-to-Interior (Case II) Cyclization Constants (in Reduced Units) Obtained from the Simulations, k_1^{BD}, and from the Theoretical Estimates, k_1^{WF}, for Unperturbed (Θ) and Excluded Volume (EV) Chains with FHI

			FHI − Θ		FHI − EV	
R_0/b	S	N	$10^2(k_1^{BD})^*$	$10^2(k_1^{WF})^*$	$10^2(k_1^{BD})^*$	$10^2(k_1^{WF})^*$
0.5	10	25	6.5 ± 0.2	6.70	2.57 ± 0.03	4.73
		45	5.85 ± 0.09	6.66	2.6 ± 0.1	4.55
		75	5.7 ± 0.2	6.44	2.5 ± 0.1	3.96
1.0	10	25	16.56 ± 0.08	14.0	9.5 ± 0.3	9.47
		45	16.0 ± 0.1	13.2	9.6 ± 0.2	8.82
		75	14.9 ± 0.1	11.3	9.18 ± 0.09	8.76
0.5	25	45	1.29 ± 0.01	1.52	0.40 ± 0.01	0.73
		75	1.19 ± 0.06	1.28	0.29 ± 0.03	0.62
1.0	25	45	2.8 ± 0.2	2.31	1.13 ± 0.02	1.12
		75	2.7 ± 0.2	2.19	1.04 ± 0.02	1.01
0.5	45	75	0.39 ± 0.05	0.52	0.102 ± 0.001	0.17
1.0	45	75	0.9 ± 0.1	0.89	0.316 ± 0.001	0.91

Table 6. Interior-to-Interior (Case III) Cyclization Constants (in Reduced Units) Obtained from the Simulations, k_1^{BD}, and from the Theoretical Estimates, k_1^{WF}, for Unperturbed (Θ) and Excluded Volume (EV) Chains with FHI

			FHI − Θ		FHI − EV	
R_0/b	S	N	$10^2(k_1^{BD})^*$	$10^2(k_1^{WF})^*$	$10^2(k_1^{BD})^*$	$10^2(k_1^{WF})^*$
0.5	10	25	5.46 ± 0.08	5.50	1.7 ± 0.2	3.33
		45	4.5 ± 0.2	4.54	1.47 ± 0.01	2.52
		75	4.32 ± 0.01	4.39	1.58 ± 0.03	2.44
1.0	10	25	12.8 ± 0.3	11.6	5.8 ± 0.3	5.72
		45	11.6 ± 0.7	10.7	5.8 ± 0.1	5.33
		75	8.86 ± 0.08	8.5	5.61 ± 0.01	5.17
0.5	25	45	0.99 ± 0.07	1.21	0.24 ± 0.01	0.53
		75	1.18 ± 0.01	1.08	0.23 ± 0.02	0.50
1.0	25	45	2.41 ± 0.09	2.02	0.56 ± 0.02	0.54
		75	1.88 ± 0.08	1.60	0.49 ± 0.09	0.48
0.5	45	75	0.43 ± 0.04	0.45	0.060 ± 0.002	0.10
1.0	45	75	0.84 ± 0.07	0.76	0.151 ± 0.004	0.15

In Tables 5 and 6 we present the results for the cyclization rate constants corresponding to FHI, in end-to-interior and interior-to-interior cases, respectively. The trend toward a limiting value of k_1 depending on S but not on N is visible once more in these tables. The ratio between simulation and theoretical estimations (data not shown) yields conclusions similar, though not completely identical, to those we have already commented. Under Θ conditions, the ratio is again close to unity. However, small fluctuations around this value can be observed which, however, do not mean deviations larger than about 20%, being in general slightly smaller in case III than in case II cyclizations. In a good solvent, we observe once more the different behavior depending on the value of R_0/b. For the larger capture radius, theory and simulation yield virtually the same results. For $R_0/b = 0.5$, the simulation constants are roughly about one-half of the theoretical values. Thus, the conclusions commented above for the validity of the theory in end-to-end cyclizations can be fully extended to the processes in which internal units are involved.

4. Summary and Conclusions

In this work we have analyzed the validity of the Wilemski−Fixman theory (through the Perico−Cuniberti formalism) to predict rate constants of intramo-

lecular reversible reactions in polymer chains. To do so, we have used a Brownian dynamics algorithm, extending previous work in our group to longer chains, and employing a more accurate algorithm. We have simulated flexible isolated chains of different molecular weights (different number of units, N), computing dynamic trajectories. Their analysis allows us the calculation of the cyclization probability as a function of time. From this function, the rate constant for the process, k_1, can be obtained, and its values compared with theoretical estimations. In addition to the usual calculation of the end-to-end cyclizations, we have also computed the rates of end-to-interior and interior-to-interior processes.

First, we have compared our simulation results computed from trajectories of unperturbed chains, with simplified treatments of hydrodynamic interactions: the free draining and the preaveraging approximations. These two cases correspond to the only situations in which the theory is able to predict results for k_1 using only analytical expressions. The comparison of simulation and theoretical results shows that the theory clearly underestimates the rate constants in these conditions. This discrepancy cannot be attributed to approximations related to the consideration of hydrodynamic interactions.

Then, we have analyzed the results corresponding to a rigorous (fluctuating) consideration of HI, both in ideal and in good solvent conditions. The theoretical estimations of the rate constants require now the use of numerical results for the correlation function $\rho(\tau)$ of the vector joining the reactive groups. Thus, the analytical character of these estimations is somehow lost. In the Θ state, the agreement between simulation and theoretical results is remarkable. The use of the numerical approximation of $\rho(\tau)$ in the analytical expressions is probably able to overcome other approximations inherent to the theory. In excluded volume conditions, on the other hand, the agreement is only partial, since it strongly depends on the capture radius of the reacting groups, R_0.

Our new results for end-to-end cyclizations mostly confirm our conclusions from previous work on shorter chains. However, the better accuracy of the algorithm used in this work has proven very useful to get more precise conclusions. In this work we have also analyzed cyclization processes involving interior units in the chain. Though the values for the rate constants are logically very different, the ratio between simulation and theoretical results produces essentially the same values we have got for the case I processes. In this sense, we can state that the theory gives the same level of approximation for the cyclization constants, no matter what the position is for the reactive beads. Throughout this work we have deliberately omitted the analysis of the molecular weight dependence of the rate constants. This analysis will be thoroughly performed in the companion paper, where the exponents of the corresponding scaling laws, $k_1 \sim S^{-\gamma}$, are compared with predictions of a new study based on the renormalization group theory.[10,11]

Acknowledgment. This work has been partially supported by Grant PB95-0384 of the DGICYT (Ministerio de Educación y Ciencia, Spain). M.O.-R. also acknowledges a Pregraduate Fellowship (Beca Colaboración) during the Academic Year 1996/1997.

References and Notes

(1) Winnik, M. A. In *Photohysical and Photochemical Tools in Polymer Science*; Winnik, M. A., Ed.; NATO ASI Series; D. Reidel: Dordrecht, The Netherlands, 1986.
(2) Wilemski, G.; Fixman, M. *J. Chem. Phys.* **1973**, *58*, 5009.
(3) Wilemski, G.; Fixman, M. *J. Chem. Phys.* **1974**, *60*, 866, 878.
(4) Yamakawa, H. *Modern Theory of Polymer Solutions*; Harper and Row: New York, 1971.
(5) Perico, A.; Cuniberti, C. *J. Polym. Sci., Polym. Phys. Ed.* **1977**, *15*, 1435.
(6) Cuniberti, C.; Perico, A. *Prog. Polym. Sci.* **1984**, *10*, 271.
(7) Perico, A.; Beggiato, M. *Macromolecules* **1990**, *23*, 797.
(8) García Fernández, J. L.; Rey, A.; Freire, J. J.; Fernández de Piérola, I. *Macromolecules* **1990**, *23*, 2057.
(9) Rey, A.; Freire, J. J. *Macromolecules* **1991**, *24*, 4673.
(10) Friedman, B.; O'Shaughnessy, B. *J. Phys. II (Paris)* **1991**, *1*, 471.
(11) Friedman, B.; O'Shaughnessy, B. *Macromolecules* **1993**, *26*, 4888.
(12) Rey, A.; Freire, J. J.; García de la Torre, J. *Polymer* **1992**, *33*, 3477.
(13) Ermak, D. L.; McCammon, J. A. *J. Chem. Phys.* **1978**, *69*, 1352.
(14) Iniesta, A.; García de la Torre, J. *J. Chem. Phys.* **1990**, *92*, 2015.
(15) Podtelezhnikov, A.; Vologodskii, A. *Macromolecules* **1997**, *30*, 6668.
(16) Horie, K.; Schnabel, W.; Mita, I.; Ushiki, H *Macromolecules* **1981**, *14*, 1422.
(17) Ushiki, H.; Horie, K.; Okamoto, A.; Mita I. *Polym. J.* **1981**, *13*, 191.
(18) Lee, S.; Winnik, M. A. *Macromolecules* **1997**, *30*, 2633.
(19) Martinho, J. M. G.; Martinho, M. H.; Winnik, M. A.; Beinert, G. *Makromol. Chem. Suppl.* **1989**, *15*, 113.

MA980254T